Self-Association of Daunomycin†

Jonathan B. Chaires, Nanibhushan Dattagupta, and Donald M. Crothers*

ABSTRACT: Daunomycin, a potent anthracycline antibiotic, self-associates in aqueous solution at concentrations greater than 10 μM. We report here visible absorbance, sedimentation equilibrium, and proton nuclear magnetic resonance (NMR) experiments that characterize this self-association. In contrast to earlier reports that the process is a simple dimerization, we find that an indefinite association model best fits our data, with an intrinsic association constant, K_i, equal to 1500 M^{-1}. From the temperature dependence of the observed NMR spectra, an enthalpy of approximately −8.0 kcal/mol is calculated. Our NMR data show that the aromatic protons of the anthracycline portion of the drug are most affected by aggregation, probably due to stacking of the anthracycline rings. Knowledge of the applicable model for the self-association process, and the equilibrium constant that describes the process, enables us to assess quantitatively the possible effects of drug aggregation on the interpretation of drug–DNA binding data. For the ionic conditions most commonly used in such studies, the amount of aggregated daunomycin will be slight and may safely be ignored.

Daunomycin (Figure 1) is an anthracycline antibiotic widely used in the treatment of various human cancers. Its chemistry and physical properties have recently been reviewed (Arcamone, 1978). In the cell, daunomycin is localized in the nucleus and is believed to act by inhibition of both DNA replication and RNA transcription.

In aqueous solution, daunomycin is reported to self-associate (Barthalemy-Clavey et al., 1974; Eksborg, 1978; Schütz et al., 1979; Martin, 1980). In these cases, concentration-dependent absorbance (Schütz et al., 1979), proton NMR[1] (Barthalemy-Clavey et al., 1974), or circular dichroism (Barthalemy-Clavey et al., 1974; Martin, 1980) spectra have been interpreted in terms of a simple dimerization model with values for the dimerization constant of 750–4000 M^{-1} reported. Aggregation beyond the dimer was deemed insignificant in most cases, although Barthalemy-Clavey et al. (1974) did suggest that further aggregation may occur at drug concentrations ≥5 mM.

Our primary interest is in the characterization of the equilibrium and kinetic constants that describe the interaction of daunomycin with DNA. Proper interpretation of such data, however, requires an understanding of the self-association of the drug, since ligand aggregation may complicate the interpretation of binding data (Bloomfield et al., 1974; Nichol & Windzor, 1972). We therefore reexamined the self-association of daunomycin in aqueous solution using visible absorbance, sedimentation equilibrium, and proton NMR measurements. Our spectroscopic measurements are in excellent agreement with those cited above; if we interpret our data in terms of a monomer–dimer model, an equilibrium constant of 3000 M^{-1} is obtained. However, sedimentation equilibrium experiments over a total drug concentration range of 0.01–2.0 mM clearly show that aggregation *beyond* the dimer is occurring. An indefinite association model adequately describes the sedimentation data; an intrinsic association constant of 1500 M^{-1} was assumed. Proton NMR measurements are consistent with such an interpretation and through the temperature dependence of selected resonances provided access to the enthalpy of the association process. In the accompanying papers, we report results from equilibrium studies on daunomycin–DNA interactions and from transient electric dichroism studies on the drug–DNA complex.

Materials and Methods

Materials. Daunomycin was obtained from Sigma Chemical Co. Deuterium oxide was Baker grade (99.75% D).

Buffers. Experiments were performed in a buffer (BPES) containing 6 mM Na_2HPO_4, 2 mM NaH_2PO_4, 1 mM EDTA, and 185 mM NaCl (pH 7.0). NMR spectra were obtained in a buffer of identical salt composition but with D_2O as a solvent (measured pH 6.8).

Absorbance Measurements. Visible absorbance spectra were recorded in either a Cary 14 or Cary 219 spectrophotometer with quartz cells of 0.1-, 1.0-, or 10.0-cm path length, as appropriate. Typically, the "auto-slit" mode was used, and measurements were at ambient temperature (22–25 °C). An extinction coefficient for the monomer of 11 500 M^{-1} cm^{-1} at 480 nm was used.

Sedimentation Equilibrium Measurements. Sedimentation equilibrium measurements were made on a Model E analytical ultracentrifuge (Spinco) equipped with a RTIC temperature control unit and a photoelectric scanner; λ = 542 nm. Sedimentation was at 29 500 rpm, 25 °C, with an AN-F rotor and 12-mm double-sector cells. Scanner traces taken at 24 and 48 h were superimposable, verifying that sedimentation equilibrium had been attained. Column heights were 6–8 mm, and the ratio of concentrations at the base of the cell to that at the meniscus was typically 1.5–3.0. The quantity $M_w(1 - \bar{v}\rho)$ was obtained from plots of ln A_{542} vs. r^2, according to

$$M_w = [2RT/(1 - \bar{v}\rho)\omega^2](\mathrm{d} \ln A_{542}/\mathrm{d}r^2)$$

where M_w is the weight-average molecular weight, R is the gas constant, T is the temperature, $\bar{v}$ is the partial specific volume, ρ is the solvent density, ω is the angular velocity of the rotor, A_{542} is the absorbance at 542 nm, and r is the radial position.

NMR. Proton NMR spectra were measured on a Brucker HX 270 MHz spectrometer interfaced to a Nicolet 1085 computer, operated in the signal-averaging mode. Data were accumulated on a Nicolet Lab 80 general signal-averaging program. Constant temperature was maintained by a Brucker Bst 100/700 temperature controller. For external lock, the

† From the Department of Chemistry, Yale University, New Haven, Connecticut 06511. *Received October 14, 1981.* Supported by National Cancer Institute Grant CA 15583 (D.M.C.) and National Institutes of Health Postdoctoral Fellowship GM 07092 (J.B.C.). Portions of this work were presented at the 1981 Meeting of the Biophysical Society (Chaires et al., 1981).

[1] Abbreviations: NMR, nuclear magnetic resonance; EDTA, ethylenediaminetetraacetic acid.

0006-2960/82/0421-3927$01.25/0

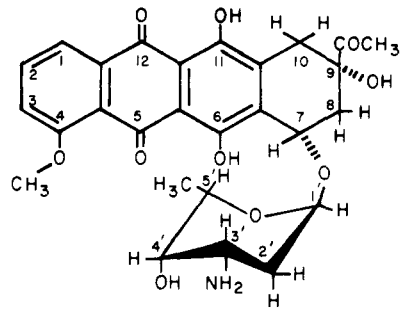

Daunomycin

FIGURE 1: Structure of daunomycin.

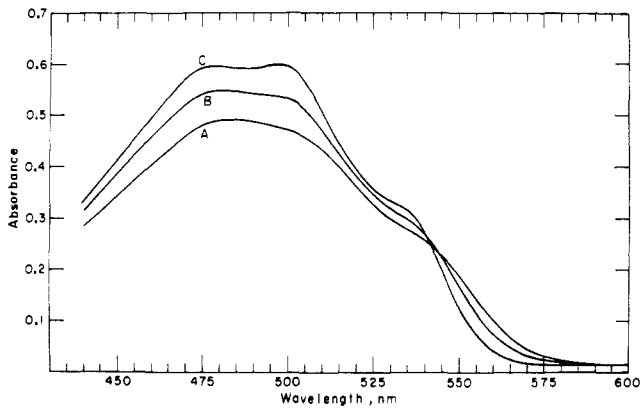

FIGURE 2: Concentration dependence of visible absorbance spectrum of daunomycin. Absorbance spectra of daunomycin solutions in 6 mM Na_2HPO_4, 2 mM NaH_2PO_4, 1 mM Na_2EDTA, and 0.185 M NaCl were recorded in a Cary 14 spectrophotometer at 25 °C: (A) 613 μM total daunomycin, 0.1-cm path length; (B) 61.3 μM total daunomycin, 1-cm path length; (C) 6.13 μM total daunomycin, 10-cm path length.

deuterated solvent was put in a coaxial tube. Chemical shifts were measured relative to the internal standard 4,4-dimethyl-4-silapentane-1-sulfonate (DSS).

Results

The first indication of daunomycin self-association comes from visible absorbance measurements, as illustrated in Figure 2. Evident is the concentration dependence of the observed absorbance spectra: upon dilution, the apparent extinction coefficient of the drug solution increases at the absorbance maximum of 480 nm, at odds with the prediction from Beer's law. An approximate isosbestic point is seen at 542–545 nm, indicating two absorbing species. Figure 3 documents the concentration dependence of the observed extinction coefficient more fully. Over the range 1–10 μM, the apparent extinction is constant at 11 500 M^{-1} cm^{-1}. Beyond 10 μM, the value of ϵ_{app} drops steadily.

Assuming a simple dimerization model

$$2D \rightleftharpoons D_2 \qquad K = [D_2]/[D]^2 \qquad (1)$$

Schwartz et al. (1970) have shown that

$$[(\epsilon_M - \epsilon)/C_0]^{1/2} = (2K/\Delta\epsilon)^{1/2}[\Delta\epsilon - (\epsilon_M - \epsilon)] \qquad (2)$$

where ϵ is the apparent extinction coefficient, ϵ_M is the extinction coefficient of the monomer, $\Delta\epsilon$ is the difference in the extinction coefficients of the monomer and dimer, K is the dimerization constant, and C_0 is the total drug concentration. Equation 2 may be used to obtain the dimerization constant, K, from the data of Figure 3. A plot of $[(\epsilon_M - \epsilon)/C_0]^{1/2}$ vs. $\epsilon_M - \epsilon$ yields an x intercept of $\Delta\epsilon$ and a slope of $(2K/\Delta\epsilon)^{1/2}$, from which K may be calculated. Such a plot is shown as an inset to Figure 2, which yields K = 3300 M^{-1}.

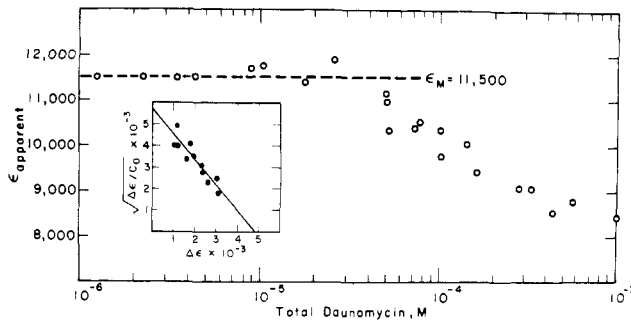

FIGURE 3: Concentration dependence of apparent extinction coefficient. The apparent extinction coefficient, $\epsilon_{app} = A_{480}/C_0$, is shown as a function of total daunomycin concentration, for samples in BPES at 25 °C. (Inset) Determination of K_{dissoc} according to eq 2.

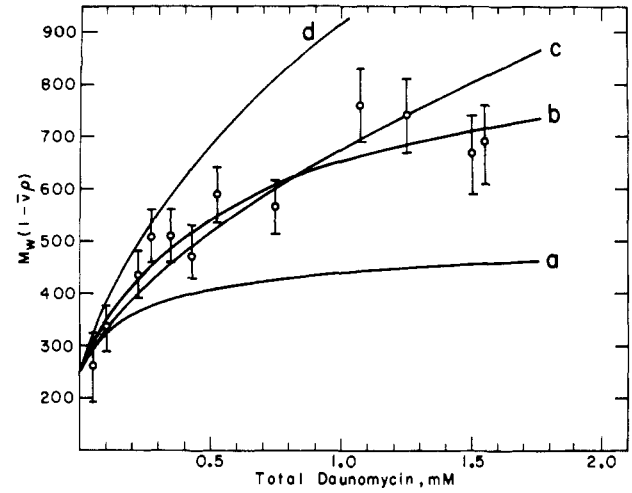

FIGURE 4: Concentration dependence of $M_w(1 - \bar{v}\rho)$ from sedimentation equilibrium experiments. Daunomycin solutions at the indicated concentrations were sedimented for at least 24 h at 30 000 rpm, 24 °C, in a buffer containing 6 mM Na_2HPO_4, 2 mM NaH_2PO_4, 1 mM EDTA, and 185 mM NaCl. The quantity $M_w(1 - \bar{v}\rho)$ is obtained from the slopes of plots of ln A_{542} vs. r^2 (see Materials and Methods). The lines were calculated for the following models, assuming a value for $\bar{v}$ of 0.5 [calculated from the known formal weight and the value of $M_w(1 - \bar{v}\rho)$ obtained at the lowest daunomycin concentration] and the indicated association constants: (a) dimer model (eq 1), K_D = 3000 M^{-1}; (b) tetramer model (eq 3), $K_1 = K_2$ = 3000 M^{-1}; (c) indefinite association model (eq 4), K_i = 1500 M^{-1}; (d) indefinite association model (eq 4), K_i = 3000 M^{-1}.

This method does not, however, provide a critical test of the dimerization model. Aggregation beyond a dimer can also account for the observed changes in extinction. Independent evidence is thus required for a definitive assignment of the association model.

Sedimentation equilibrium experiments can, in principle, provide the needed evidence. If the association of daunomycin is a simple dimerization, the weight-average molecular weight should approach a limiting value of twice the monomer molecular weight as the total drug concentration is increased. Figure 4 shows that this is *not* the case. Figure 4 shows a plot of the quantity $M_w(1 - \bar{v}\rho)$ as a function of total drug concentration. Curve a is the calculated behavior for a dimerization model with a dimerization constant close to the value obtained from the data in Figure 3, adjusting $\bar{v}$ for best fit to the low-concentration data. The experimental results are inconsistent with this model; at a total drug concentration of 0.5 mM, the value of $M_w(1 - \bar{v}\rho)$ has already exceeded the limiting value predicted by the dimer model and continues to rise as the concentration is increased further. The inconsistency is not in the choice of K, since the critical prediction is

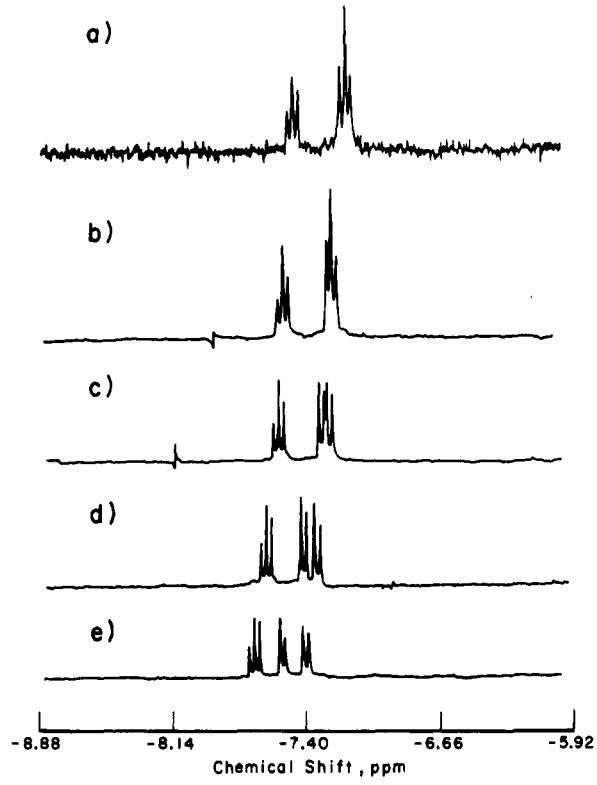

FIGURE 5: Concentration dependence of chemical shifts of protons H1, H2, and H3. Portions of the 270-MHz ^1H NMR spectrum (relative to DSS) are shown for the following total daunomycin concentrations: (a) 7 mM, 25 °C; (b) 7 mM, 50 °C; (c) 4.7 mM, 50 °C; (d) 2.35 mM, 50 °C; (e) 1.18 mM, 50 °C.

that a limiting value of $M_w(1 - \bar{v}\rho) = 500$ will not be exceeded. Choosing an equilibrium constant larger than 3000 M^{-1} simply produces curves that reach this limiting value at lower total drug concentrations.

We next considered models that include aggregation beyond the dimer. First, the formation of a tetramer was considered, following the scheme

$$2D \rightleftharpoons D_2 \qquad K_1 = [D_2]/[D]^2 \tag{3}$$
$$2D_2 \rightleftharpoons D_4 \qquad K_2 = [D_4]/[D_2]^2$$

An adequate fit to the data in Figure 4 is seen with $K_1 = K_2 = 3000\ M^{-1}$ (curve b). However, the data are fit essentially as well with an indefinite association model:

$$\begin{aligned} 2D &\rightleftharpoons D_2 & K_1 &= [D_2]/[D]^2 \\ D + D_2 &\rightleftharpoons D_3 & K_2 &= [D_3]/([D_2][D]) \\ &\vdots \quad \vdots & & \\ D + D_{n-1} &\rightleftharpoons D_n & K_n &= [D_n]/([D_{n-1}][D]) \\ & K_1 = K_2 = \ldots = K_n = K_i & & \end{aligned} \tag{4}$$

assuming an intrinsic association constant $K_i = 1500\ M^{-1}$, with 30% uncertainty (Figure 4, curve c). Significantly higher values of K_i do not fit the data (curve d). With the scatter in our experimental data, we cannot rationally choose between the indefinite association or the more limited monomer–tetramer model. Indeed, even with data of higher precision, it may be a hopeless task to distinguish between the two models (van Holde et al., 1969). It is clear, however, that a simple monomer–dimer model cannot account for the data in Figure 4 and that higher aggregation must occur.

We next examined the concentration dependence of the proton NMR spectrum of daunomycin in D_2O. We based our assignments on those reported by Arcamone et al. (1968), who

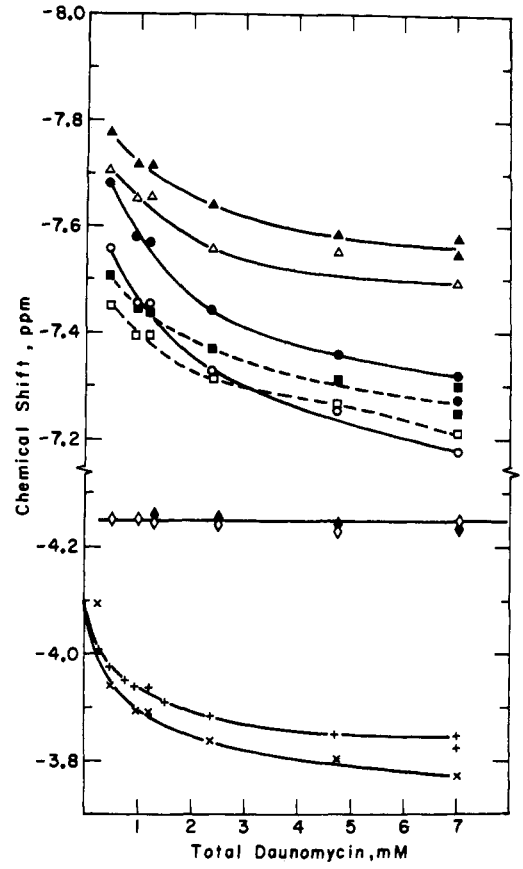

FIGURE 6: Concentration dependence of chemical shifts for selected resonances. In all cases, open symbols refer to 25 °C and closed symbols refer to 50 °C for the following protons: H1 (○, ●); H2 (△, ▲); H3 (□, ■); H7 (◇, ◆); O–CH_3 [25 °C (×), 50 °C (+)].

reported data for *N*-acetyldaunomycin in chloroform. Our D_2O spectra differ from the reported chloroform spectra in several important respects. The most downfield resonance in D_2O is a triplet, which we assign to the proton H2, whereas a doublet (assigned to H1) is most downfield in chloroform. Figure 5 illustrates this, along with the concentration dependences of these ring proton resonances. We have been unable to assign unambiguously the doublets seen in Figure 5. We assume that the most downfield doublet (at low concentration) belongs to H1 and that it will, at infinite dilution, cross the H2 triplet. Nuss et al. (1980) have assigned the resonances for H1, H2, and H3 in D_2O and in fact find that H1 is the most downfield doublet at infinite dilution.

Figure 6 illustrates the changes in the chemical shifts of selected resonances with changes in the total drug concentration. The resonances for H1, H2, H3, H7, and O–CH_3 are shown. The chemical shift for H7 is independent of concentration, while a steady shift downfield may be seen in the other cases.

By use of the formalism of Dimicoli & Hélène (1973), the data of Figure 6 may, in priniciple, be used to obtain an association constant. For a monomer–dimer model, they show that

$$(\Delta\sigma/C_0)^{1/2} = (2K/\Delta\sigma_D)^{1/2}(\Delta\sigma_D - \Delta\sigma) \tag{5}$$

while for an indefinite association model

$$(\Delta\sigma/C_0)^{1/2} = [K/(2\Delta\sigma_D)]^{1/2}(2\Delta\sigma_D - \Delta\sigma) \tag{6}$$

where $\Delta\sigma$ is the difference between the observed chemical shift and the chemical shift of the monomer, $\Delta\sigma_D$ is the difference in chemical shift between the monomeric and dimeric forms, assumed in eq 6 to be half the chemical shift of the infinite

Table I: Estimation of σ_M, σ_D, σ_A, and K from Equations 7 and 8[a]

	plot according to eq 7		plot according to eq 8		
resonance	σ_M (ppm)	σ_D (ppm)	σ_A (ppm)	σ_M (ppm)	K' (M^{-1})
H1	8.12	7.66	7.2	8.06	1538
H2	8.04	7.77	7.51	7.99	1515
H3	7.80	7.51	7.23	7.80	1523
O-CH_3	4.18	3.98	3.78	4.14	1120

[a] The data in Figure 6, along with an initial estimate of $K = 1500$ M^{-1}, were used in an algorithm described in the text to estimate the chemical shift of the monomer, dimer, and aggregate and to confirm the estimate of K. σ_A is the chemical shift of the aggregate form.

aggregate, K is the intrinsic association constant, and C_0 is the total drug concentration. A value for the chemical shift of the monomer is required to use eq 5 or 6, usually obtained by extrapolation of data such as illustrated in Figure 6 to zero concentration. However, if our estimate of K from sedimentation equilibrium experiments is correct, at the lowest concentration we were able to use for NMR experiments (~0.5 mM), only 46% of the drug exists as free monomer in solution. We therefore have sought an alternative to the risky and somewhat arbitrary extrapolation required to use eq 6.

If eq 6 is squared, straightforward algebraic manipulation leads to

$$\sigma(1/C_0 + 2K) = \sigma_M/C_0 + 2K\sigma_D + K(\sigma - \sigma_M)^2/[2(\sigma_D - \sigma_M)] \quad (7)$$

where σ_M is the chemical shift of the monomer, σ is the observed chemical shift, and σ_D is the chemical shift of the dimer. By the assumptions made in obtaining eq 6, the chemical shift σ_A of the aggregated drug is $2(\sigma_D - \sigma_M) + \sigma_M$. If a value for K is known (or assumed), a plot of $1/C_0 + 2K$ vs. $1/C_0$ should produce a linear plot with a slope of σ_M and an intercept of $2K\sigma_D$ [at the intercept, $\sigma - \sigma_M = 2(\sigma_D - \sigma_M)$]. Multiplication of both sides of eq 7 by C_0 and further algebraic rearrangement yields

$$\sigma(1 + 2KC_0) - KC_0(\sigma - \sigma_M)^2/[2(\sigma_D - \sigma_M)] = \sigma_M + 2KC_0\sigma_D \quad (8)$$

where the symbols have been previously defined. A plot of the left side of eq 8 vs. C_0 should yield a slope of $2K\sigma_D$ and an intercept of σ_M. We have used eq 7 and 8 in the following algorithm. First, we used our estimate of K from sedimentation equilibrium experiments and the data of Figure 6 to construct a plot according to eq 7. A linear least-squares fit was used to obtain the slope and intercept, which yielded σ_M and σ_D. These quantities, along with the same value of K, were used to construct a plot according to eq 8. Least-squares fitting yielded an intercept of σ_M and a slope of $2K\sigma_D$. The results are shown in Table I. Assuming an indefinite association model with $K = 1500$ M^{-1} provides a self-consistent set of values for σ_M from the two plots and returns a value of K from eq 8 in close agreement with the initial estimate of K. In principle, the estimate could be refined by iteration although we have not done so. The results shown in Table I indicate that our NMR data are consistent with the association model and equilibrium constant obtained from sedimentation equilibrium experiments.

Table II compares our values for the chemical shifts of selected resonances to those reported by other laboratories. The general agreement is quite good; in particular, the D_2O results at infinite dilution are in close agreement with the chemical shifts found in $CDCl_3$, a solvent in which self-association would be minimal.

Table II: Observed Chemical Shifts for Selected Resonances

resonance				sol-	com-	
H1	H2	H3	O-CH_3	vent	ments	reference
8.1	7.9	7.8	4.1	D_2O	*a*	this work
8.04	7.79	7.65		$CDCl_3$		
7.87	7.83	7.61	4.07	D_2O	*b*	Nuss et al. (1980)
7.680	7.755	7.465	3.965	D_2O	*c*	Patel (1980)
8.0	7.77	7.36	4.04	$CDCl_3$		Arcamone et al. (1968)

[a] At infinite dilution, estimated from eq 7 and 8, assuming $K = 1500$ M^{-1}. [b] Infinite dilution. [c] 2 mM daunomycin in 0.1 M phosphate-1 mM EDTA, 90 °C.

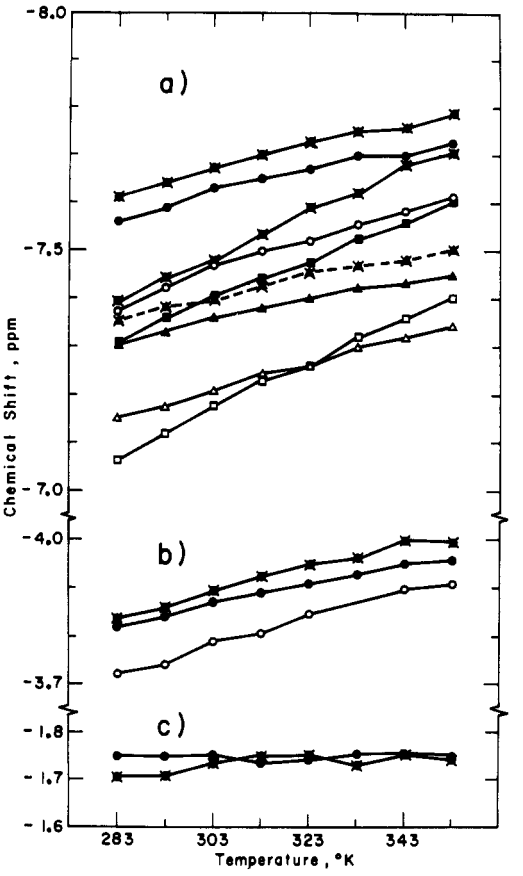

FIGURE 7: Temperature dependence at chemical shifts for selected resonances. Ring protons (a) H1 (○, ●, crossed ●), H2 (△, ▲, crossed ▲), and H3 (□, ■, crossed □), (b) O–CH_3 (○, ●, crossed ○), and (c) CO–CH_3 (●, crossed ○), at total drug concentrations of 7, 1.5, and 0.74 mM, respectively.

Figure 7 shows the temperature dependence of the observed chemical shifts for several resonances at fixed total drug concentration. Such data may be used to provide access to the enthalpy of the association reaction. For the indefinite association model, the concentration of monomer is given by (Meyer & van der Wyk, 1937)

$$C_M = (1/K)[2KC_0 + 1 - (4KC_0 + 1)^{1/2}]/(2KC_0) \quad (9)$$

where C_M is the molar monomer concentration and the other symbols have been previously defined. If we define the fraction of monomeric drug α by

$$\alpha = C_M/C_0 = 1 - (\sigma_M - \sigma_{obsd})/(\sigma_M - \sigma_A)$$

eq 9 may be recast into the form

$$\alpha = [1/(KC_0)][2KC_0 + 1 - (4KC_0 + 1)^{1/2}]/(2KC_0) \quad (10)$$

Table III: Comparison of Reported Equilibrium Constants for Daunomycin Self-Association

no.	K (M^{-1}) dimer model	K (M^{-1}) indefinite association model	method	conditions	reference
1a	3300		absorbance	BPES	this work
1b		1500	SE	BPES	
1c	760	1510	NMR	BPES	
2a	700	1400	NMR	1.5 mM sodium citrate, 15 mM NaCl, pH 7.0	Barthalamey-Clavey et al. (1974)
2b	570		CD		
3	4500		absorbance	200 mM ionic strength, pH 6	Shütz et al. (1979)
4	6400		absorbance, CD	10 mM phosphate, pH 7.3, 25 °C	Martin (1980)
	9115			12 °C	
	5235			37 °C	
	11600			0.5 M NaCl	

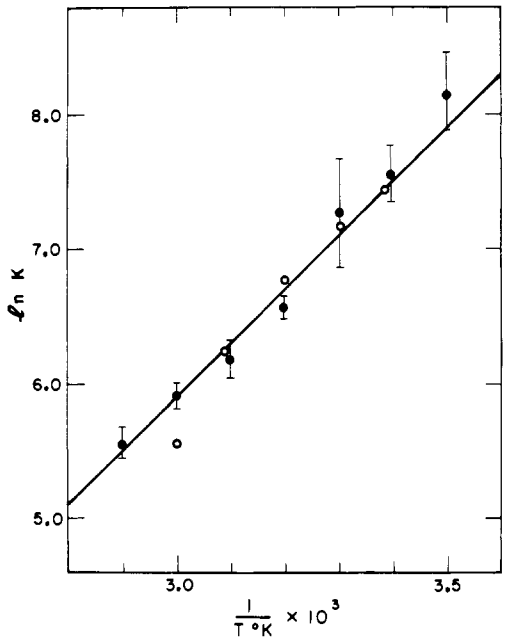

FIGURE 8: Determination of enthalpy of association with van't Hoff plot. Data from the NMR experiments of Figure 7 (●) or visible absorbance measurements (○) were used to calculate K_i. The slope yields $\Delta H^\circ = -7.98$ kcal/mol.

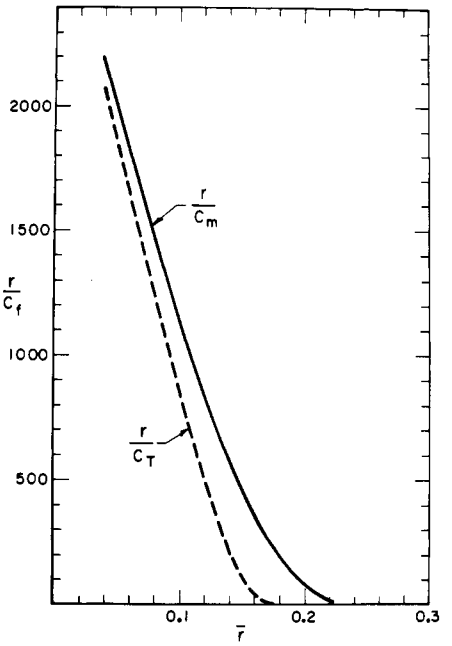

FIGURE 9: Effect of daunomycin aggregation on a Scatchard plot of binding data.

Equation 10 may then be used to estimate K from the experimental data of Figure 7. At each temperature, α was determined from the experimental data, and K was then calculated from eq 10. Figure 8 shows the van't Hoff plot that results. The plot appears linear, with a slope yielding $\Delta H^\circ = -8.0 \pm 1$ kcal/mol. In an independent experiment, a sample of daunomycin at 88 μM was monitored at 480 nm while continuously heating the sample. By analogy with the above definition of α, the optical data may be analyzed by defining

$$\alpha = 1 - (\epsilon_M - \epsilon_{obsd})/(\epsilon_M - \epsilon_A)$$

with $\epsilon_M = 11\,500$ M^{-1} cm^{-1} and the aggregate form extinction coefficient $\epsilon_A = 6725$ M^{-1} cm^{-1}. Again, eq 8 may be used to estimate K. The results are shown as the open circles in Figure 9, and the agreement with the independently obtained NMR data is excellent. Assuming $\Delta H^\circ = -8.0$ kcal/mol at 25 °C and $\Delta G^\circ = -RT \ln K = -4.3$ kcal/mol (25 °C), we estimate an entropy, ΔS°, of −14.3 eu for the association process.

Discussion

Our sedimentation equilibrium results show that daunomycin aggregates beyond a dimer. An indefinite association model with an association constant of 1500 M^{-1} adequately fits the sedimentation data, as well as the independently gathered proton NMR data. An enthalpy of −8.0 kcal/mol and an entropy of −14.3 eu (25 °C) are obtained from the temperature dependence of the NMR spectra. Thus at room temperature the association is driven largely by enthalpic contributions.

Thermodynamic values such as these are characteristics of a reaction involving the stacking of planar aromatic rings. Other compounds with planar aromatic structures have been shown to associate according to the same indefinite association model we favor for daunomycin, with similar equilibrium and thermodynamic constants. For example, Braswell & Lary (1981) have found values of $K = 600$ M^{-1} and $\Delta H^\circ = -10.0$ kcal/mol for the aggregation of methylene blue and $K = 2000$ M^{-1} and $\Delta H^\circ = -8.9$ kcal/mol for the aggregation of acridine orange, in 0.1 M triethanolamine. In both cases, the equilibrium constants refer to an indefinite association model, and the enthalpy has been calculated by us from the data presented by Braswell & Lary. Previous results from this laboratory on the solution behavior of the antibiotic actinomycin (Crothers et al., 1968) have, however, favored a dimerization model for that drug, with $K = 10^3$ M^{-1}, $\Delta H^\circ = -15$ kcal/mol, and $\Delta S^\circ = -38$ eu.

Comparison of our data on daunomycin self-association with those previously reported is facilitated by inspection of Table III. Different models for the association process have been

used, making direct comparison of the equilibrium constants difficult. To facilitate comparison, we present our data for both models. Our primary spectroscopic and NMR data are in excellent agreement with those previously reported, given the slight differences in ionic conditions. This is reflected in the close agreement of the equilibrium constants in Table III. Our sedimentation equilibrium experiments vitiate the monomer–dimer model and lead us to favor an indefinite association model. Recasting the NMR data of Barthalemy-Clavey et al. in terms of this model again yields a value for the equilibrium constant in good agreement with the value we have found.

Our NMR data give some insight into the structure of the daunomycin aggregate. The ring protons H1/H3, H2, and O–CH_3 are the most concentration-dependent resonances, while the resonances for H7, $COCH_3$, and most of the sugar protons are largely independent of concentration. Stacking of the anthracycline ring system, with concomitant ring current shifts, is consistent with these observations. Supposing a stack in which the sugar portion of the drug forms a helical arrangement on the periphery of the stacked anthracycline rings, there would be no steric reasons for limited aggregates.

We now assess the effect of self-association on the interpretation of daunomycin–DNA binding data. In a typical binding experiment, one determines $\bar{r}$, the amount of drug bound per base pair of DNA, and C_f, the molar concentration of free drug. If the drug self-aggregates, the latter quantity will be overestimated and the standard state incorrectly identified. C_f may erroneously be assigned to C_M, the molar concentration of monomer. The two quantities are related by

$$C_f = \alpha C_T + C_M$$

where C_T is the fraction of total free drug in aggregated form. To extract binding parameters for the interaction of a drug with DNA, one typically plots according to the formalism of McGhee & von Hippel (1974)

$$\bar{r}/C_M = K_{app}(1 - n\bar{r})[(1 - nr)/[1 - (n - 1)r]]^{n-1}$$

where $\bar{r}$ and C_M have been defined and K_{app} and n are the binding constant and the exclusion parameter, respectively. If the drug self-aggregates, the quantity r/C_M is an underestimate of r/C_f

$$r/C_f = (r/C_M)/(1 + \alpha C_T)$$

where the symbols all have been previously defined. Figure 9 illustrates the difficulties for a particular case. With a binding constant of comparable magnitude to that for the self-association of the drug, equating r/C_f with r/C_M is seen to lead to considerable error in the Scatchard plot: a pronounced shift in the x intercept, which is used to obtain n, is the most serious error in this particular case. In more dramatic cases, neglect of self-association may lead to pronounced curvature in cases where linear plots truly describe the experimental data (Bloomfield et al., 1974). At 200 mM ionic strength, daunomycin binds to DNA with an association constant of around 10^6 M^{-1}. Calculations show that with such tight binding the free drug concentrations are so low that self-association will not interfere with the interpretation of the binding data and that plots such as in Figure 9 will not need correction. Self-association may for all practical purposes be ignored for these conditions. At other, higher, salt conditions, the aggregation of the drug is enhanced (Martin, 1980; our results, data not shown), while the affinity of the drug for DNA is decreased, which may lead to the difficulties we have discussed. Finally, at the high drug concentrations required for NMR studies on daunomycin–DNA interactions (Nuss et al., 1980; Patel, 1980), aggregation is certain to be a problem. The results presented here provide the means for making appropriate corrections in these cases.

References

Arcamone, F. (1978) *Top. Antibiot. Chem. 2*, 102–237.

Arcamone, F., Cassinelli, G., Franceschi, G., & Orezz, P. (1968) *Tetrahedron Lett. 30*, 3353–3356.

Barthalemy-Clavey, V., Maurizot, J. C., Dimicoli, J. L., & Sicand, P. (1974) *FEBS Lett. 46*, 5–10.

Bloomfield, V., Crothers, D. M., & Tinoco, I. (1974) *Physical Chemistry of Nucleic Acids*, pp 411, Harper and Row, New York.

Braswell, E., & Lary, J. (1981) *J. Phys. Chem. 85*, 1573–1578.

Chaires, J. B., Dattagupta, N., & Crothers, D. M. (1981) *Biophys. J. 33*, 314a.

Crothers, D. M., Sabol, S. L., Ratner, D. I., & Müller, W. (1968) *Biochemistry 7*, 1817–1822.

Dimicoli, J.-L., & Hêlêne, C. (1973) *J. Am. Chem. Soc. 95*, 1036–1044.

Eksborg, S. (1978) *J. Pharm. Sci. 67*, 782–785.

Martin, S. R. (1980) *Biopolymers 19*, 713–721.

McGhee, J., & von Hippel, P. (1974) *J. Mol. Biol. 86*, 469–489.

Meyer, K. H., & van der Wyk, A. (1937) *Helv. Chim. Acta 20*, 1321.

Nichol, L., & Windzor, D. J. (1972) *Migration of Interacting Systems*, Clarendon Press, Oxford.

Nuss, M. E., James, T. L., Apple, M. A., & Kollman, P. A. (1980) *Biochim. Biophys. Acta 609*, 136–147.

Patel, D. (1980) in *Nucleic Acid Geometry and Dynamics* (Sarma, R. H., Ed.) p 224, Pergamon Press, New York.

Schütz, H., Gollmick, F. A., & Stutter, E. (1979) *Stud. Biophys. 75*, 147–159.

Schwartz, G., Klose, S., & Balthasan, W. (1970) *Eur. J. Biochem. 12*, 454–460.

van Holde, K. E., Rossetti, G. P., & Dyson, R. D. (1969) *Ann. N.Y. Acad. Sci. 164*, 279–293.